Nickel and copper deposition on fine alumina particles by using the chemical vapor deposition-circulation fluidized bed reactor technique

YEE-WEN YEN, SINN-WEN CHEN
Department of Chemical Engineering, National Tsing-Hua University, Hsin-Chu, Taiwan 30043, Republic of China

A Chemical Vapor Deposition-Circulation Fluidized Bed Reactor technique has been developed to deposit metallic Ni and Cu onto alumina particles of 45 μm diameter. The furnaces consisted of upper and lower zones, and the deposition precursors were produced both *in situ* and by vaporization of chlorides. X-ray diffraction, metallographical examination, and compositional analysis were used to analyze the deposition layers. For both Ni and Cu deposition, the deposition rates increased with higher temperatures of the lower furnace. The rates increased with greater amounts of chloride addition as well, but they reached plateaus when the amounts of addition were more than 40%. © *2000 Kluwer Academic Publishers*

1. Introduction

Surface treatment of materials is a very common engineering practice. Different surface treatment techniques have been developed to meet the various engineering requirements of materials; for instance, to increase surface hardness, to increase wettability, and to reduce oxidation rate. Surface treatment can be conducted via liquid routes, such as painting, hot dipping, sol-gel processing, and electroplating. Recent efforts are to modify the surfaces of materials by using "dry" techniques including ion implantation, physical vapor deposition (PVD), chemical vapor deposition (CVD), etc. [1–4]

Blocher was the first investigator to carry out chemical vapor deposition by using a fluidized bed as a reactor, which was granted a patent [5]. Various studies have been conducted to perform surface treatment by using the chemical vapor deposition-fluidized bed reactor (CVD-FBR) technique [3–19]. By using the CVD-FBR technique and in situ generating the deposition precursor, Chen *et al.* [3, 4] was able to deposit Ni, Cu, Ti onto alumina and SiC substrates. However, the size of the particles used in Chen et al's studies was about 250 μm, which might sometimes be too large for applications. But if alumina particles of smaller sizes had been used in the CVD-FBR process, elutriation of particles would have occurred during fluidization. To overcome the elutriation problems of fine particles, a circulation fluidized-bed reactor (CFBR), rather than the fluidized-bed reactor, has been used in this study to conduct Ni and Cu deposition onto finer alumina particles.

2. Experimental Procedure

The experimental apparatus is shown in Fig. 1. The stainless steel gas mixer was wrapped with a heating pad. The inlet gases, Ar, H$_2$ and HCl gases, were mixed and preheated to 250°C in the gas mixer before they were introduced into the reactor. The reactor consisted of a quartz main body and a Pyrex glass cyclone. The outside and the inside diameters of the quartz reactor were 2.4 cm and 2.2 cm, respectively, with the length of 75 cm. The Pyrex glass cyclone was designed to collect the alumina particles which were elutriated in fluidization.

The gas distributor was also made of quartz. The metal packed bed was 5 cm high and sat on the distributor. The alumina particles were loaded on top of the metal bed and their size was 45 μm in diameter. The reactor was first purged with Argon gas, and then heated to the pre-determined temperatures. The furnace had two zones. The temperature range of the upper furnace was 675–800°C, and that of the lower furnace was 725–800°C. When the temperatures of the upper and lower furnaces reached the predetermined temperatures, the HCl and H$_2$ gases began to be introduced into the reactor together with the argon gas. The composition of the inlet gas was 8.3 vol.% HCl, 28.4 vol.% H$_2$, and 63.3 vol.% Ar. The superficial velocity was 10.9 cm/s. Besides pure alumina particles, certain amounts of metal chlorides were also added together in some experiments to study their effects upon metal depositions. The diameters of the chlorides were 250 μm. The experimental conditions of the CVD-CFBR experiments are summarized in Table I.

After 3 hours' reaction, the power of the furnace was turned off, the inlet of HCl gas was stopped, and the quartz reactor cooled down with the flow of hydrogen and argon gases. When the system cooled down to the room temperature, then both the inlet of H$_2$ and argon gases were stopped, and the alumina particles were taken out of the reactor. The surface morphology and the compositions of the deposits of the alumina particles

TABLE I Summary of the CVD-CFBR experimental conditions

|	Metal	Temperature of upper furnace	Temperature of lower furnace	Addition of metal chloride	Reaction time
1	Ni	675°C	785°C	5 wt% NiCl$_2$	3 hours
2	Ni	675°C	775°C	5 wt% NiCl$_2$	3 hours
3	Ni	675°C	800°C	5 wt% NiCl$_2$	3 hours
4	Ni	675°C	785°C	None	3 hours
5	Ni	675°C	775°C	None	3 hours
6	Ni	675°C	800°C	None	3 hours
7	Ni	675°C	785°C	10 wt% NiCl$_2$	3 hours
8	Ni	675°C	785°C	20 wt% NiCl$_2$	3 hours
9	Ni	675°C	785°C	40 wt% NiCl$_2$	3 hours
10	Ni	675°C	785°C	50 wt% NiCl$_2$	3 hours
11	Ni	685°C	785°C	5 wt% NiCl$_2$	3 hours
12	Ni	700°C	785°C	5 wt% NiCl$_2$	3 hours
13	Ni	725°C	785°C	5 wt% NiCl$_2$	3 hours
14	Ni	750°C	785°C	5 wt% NiCl$_2$	3 hours
15	Ni	785°C	785°C	5 wt% NiCl$_2$	3 hours
16	Cu	675°C	725°C	5 wt% CuCl	3 hours
17	Cu	675°C	775°C	5 wt% CuCl	3 hours
18	Cu	675°C	775°C	10 wt% CuCl	3 hours
19	Cu	675°C	775°C	20 wt% CuCl	3 hours
20	Cu	675°C	775°C	40 wt% CuCl	3 hours
21	Cu	675°C	775°C	50 wt% CuCl	3 hours
22	Cu	700°C	775°C	5 wt% CuCl	3 hours
23	Cu	750°C	775°C	5 wt% CuCl	3 hours
24	Cu	775°C	775°C	5 wt% CuCl	3 hours
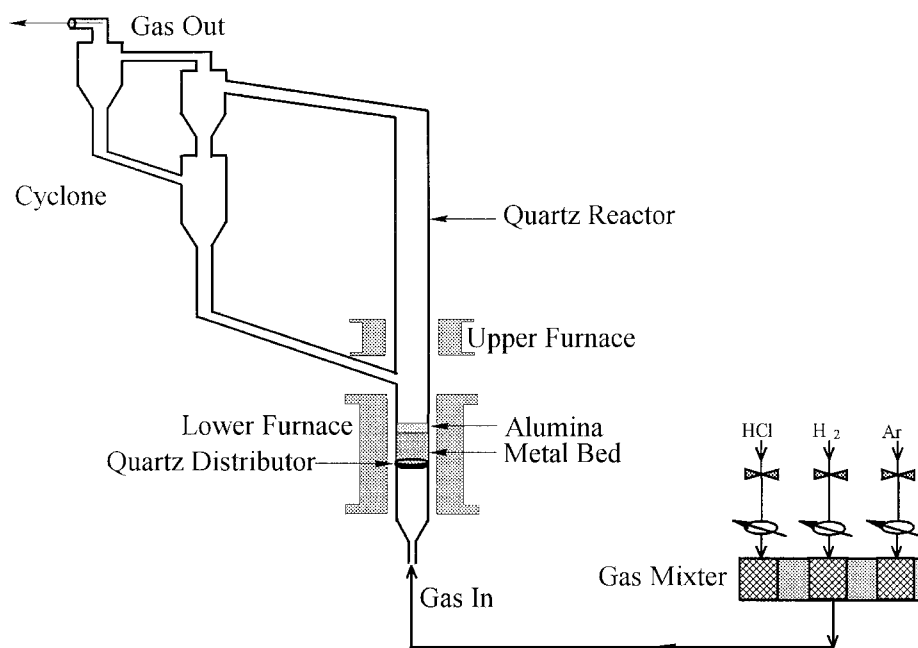
Figure 1 A schematic diagram of the CVD-CFBR apparatus.

were analyzed by using SEM (scanning electron microscopy) with EDS (energy dispersive spectrometer). XRD (X-ray diffraction) analysis was also used in the identification of the deposits. The thickness of the deposition layers on the alumina particles was calculated based on the compositional analysis results determined by using ICP-AES (inductively coupled plasma-atomic emission spectrometer).

3. Results and discussion
At the gas velocity of 10.9 cm/s, alumina particles were elutriated from the top of the reactor and carried into the cyclone region. The gas velocity decreased in the cyclone region, and it was observed that the elutriated particles settled and flowed downward back to the reactor. The originally brownish alumina particles turned into a dark gray color after 3 hours' reaction with the following experimental condition: 5 wt% NiCl$_2$ was put together with the alumina particles, the temperatures of the upper furnace was 675°C and that of the lower furnace was 785°C. Shown in Fig. 2 is the composition of the dark gray deposit analyzed by using EDS, which indicates that the deposit contains nickel element. The result of the XRD analysis shown in Fig. 3 further confirms the successful deposition of metallic nickel on
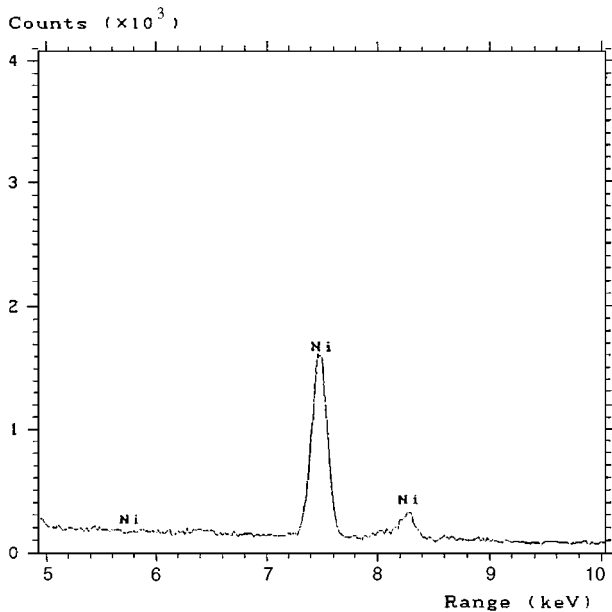
Figure 2 The EDS compositional analysis of the Ni-deposited alumina particle from experiment 1.

Figure 3 The XRD result of the Ni-deposited alumina particles from experiment 1.

the alumina particles. Fig. 4 is the nickel elemental X-ray mapping graph which demonstrates that the deposition of nickel on the alumina particles is uniform, while the SEM secondary electron image micrograph reveals that the surface morphology of the deposits is wavy as shown in Fig. 5.

The thickness of the deposition layer is determined by the following procedures. Proper amounts of Ni-deposited alumina particles were weighed. These particles were then soaked in acid to dissolve the Ni-layer. The acid solution was diluted according to the standard analytical chemistry procedures. The concentration of Ni in the acid solution was determined by using ICP-AES, and the amount of dissolved nickel (w_{Ni}) was calculated from the ICP-AES result. By assuming the alumina particles are spheres of 45 μm diameter and the thickness of the deposition layer (ΔR) is much smaller than the diameter, the thickness (ΔR) can be calculated with the following equation:

$$\text{Ni wt\%} = \frac{w_{Ni}}{w_{Ni} + w_{Al_2O_3}} = \frac{3 \Delta R \rho_{Ni}}{3 \Delta R \rho_{Ni} + R \rho_{Al_2O_3}} \quad (1)$$

where the 22.5 μm R is the radius of the particles, and the ρ_{Ni} and $\rho_{Al_2O_3}$ are densities of nickel and alumina, and are 8.90 g/cm^3 and 4.0 g/cm^3, respectively. After 3 hours' reaction in the experimental condition mentioned above, there are 2.81 mg Ni deposited on the 101.6 mg Ni-deposited alumina particles, i.e. w_{Ni} is 2.81 mg and ($w_{Ni} + w_{Al_2O_2}$) is 101.6 mg. The thickness of the deposited layer can then be calculated by using Equation 1 and it is 0.1 μm.

As summarized in Table I, experiments 2 and 3 also deposited Ni onto the alumina particles by using the CVD-CFBR technique with almost identical experimental conditions as used in experiment 1. The only difference was that the temperatures of the lower furnace were higher in experiments 2 and 3 and were 775°C and 800°C, respectively. Similar results were obtained
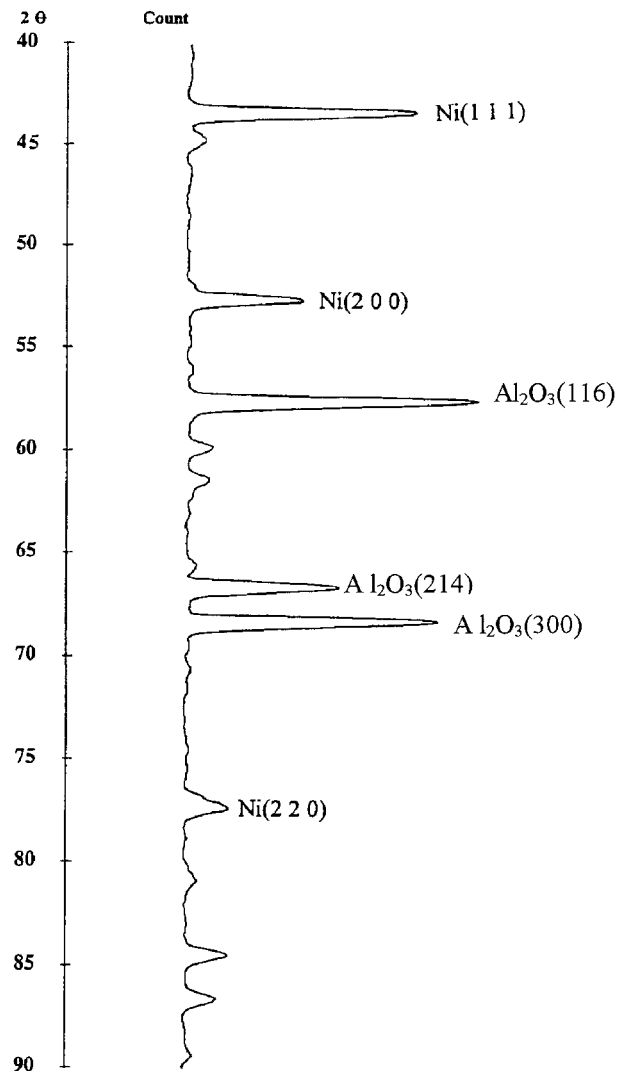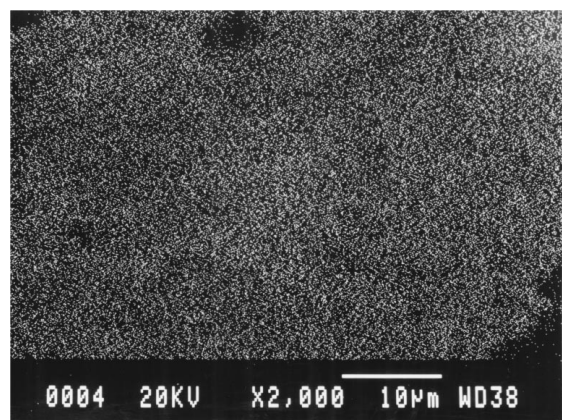

Figure 4 The elemental Ni X-ray mapping of the Ni-deposited alumina particle from experiment 1.

in these three experiments. The brownish alumina particles turned into dark gray color with the deposition of metallic Ni. As shown in Fig. 6 for experiments 1–6, the thickness of the deposition layer increased as the temperatures of the lower furnace rose if all other processing conditions were kept identical and the reaction time was 3 hours as well. It is expected because the lower furnace is the formation region of the deposition
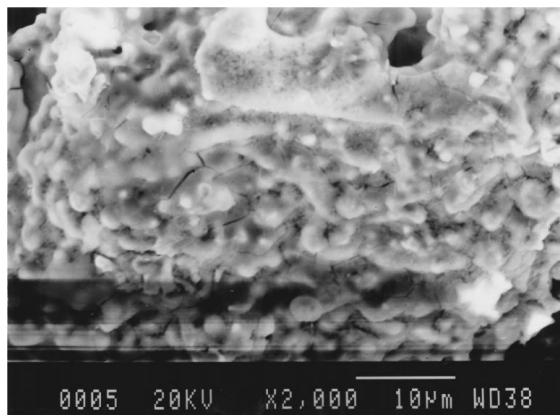
1441

Figure 5 The SEM secondary electron image of surface morphology of the Ni-deposited alumina particle from experiment 1.
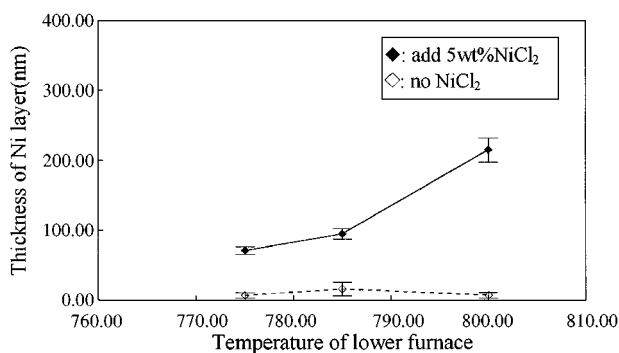

Figure 6 The relation between the thickness of the deposition layer and the temperature of the lower furnace. The temperature of the upper furnace is 675°C.
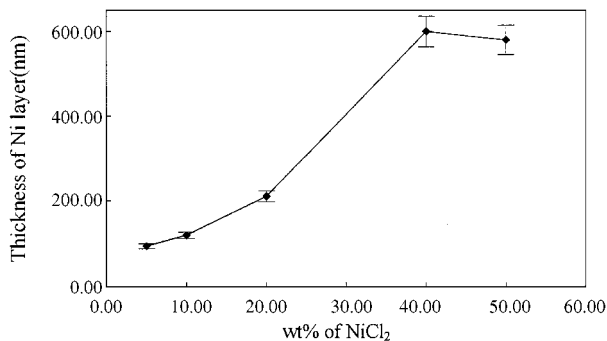

Figure 7 The relation between the thickness of the deposition layer and the amount of $NiCl_2$ addition. The temperature of the upper furnace is 675°C and that of the lower furnace is 785°C .
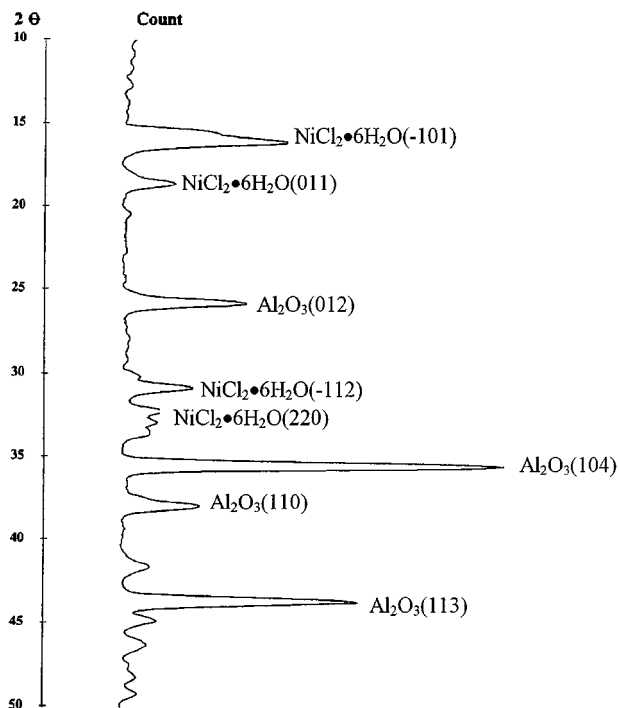

Figure 8 The XRD result of the yellow-color deposits from experiment 14.

precursor. Experiments with higher lower furnace temperatures would have higher precursor formation rates, and thus their deposition rates would be higher.

It was observed by using SEM with EDS that metallic Ni also successfully deposited on the alumina particles from the CVD-CFBR experiments without adding any $NiCl_2$; however, as shown in Fig. 6 the thickness of the deposition layer was much smaller than that of those with the addition of $NiCl_2$. Since the thickness of the layers obtained from the experiments without adding $NiCl_2$ was very small and the relative errors of the thickness measurements were large, the temperature effect upon the deposition layer growth could not be determined from these thickness data. As shown in Fig. 7 for experiments 1 and 7–10, the thickness of the deposition layer increased with the amount of $NiCl_2$ addition, and the thickness reached a plateau when the $NiCl_2$ addition was about 40 wt%. The $NiCl_2$ powders coagulated and blocked the gas flow during heating when the amount of $NiCl_2$ addition was more than 40 wt%. It is likely that higher amount of $NiCl_2$ addition increased the amount of $NiCl_2$ vapor in the alumina fluidized bed region and thus increased the rate of Ni deposition; however, when the $NiCl_2$ addition was more than 40 wt%, the effect of coagulation was severe and the flow rate of gas into the reactor was significantly reduced. Thus the amount of $NiCl_2$ vapor in the alumina fluidized bed region was in fact not increased even if more than 40 wt% $NiCl_2$ was added.

Similar to experiment 1, nickel metal were successfully deposited on the alumina particles for all the CVD-CFBR experiments 11–15. Experiments 1 and 11–15 were carried out at a fixed temperature 785°C in the lower furnace, while the temperatures of the upper furnace were 675°C, 685°C, 700°C, 725°C, 750°C and 785°C, respectively. However, for the experiments 14 and 15, deposits of a yellow color were found on the inner walls of the quartz reactor and the Pyrex cyclone. The XRD results shown in Fig. 8 indicates these yellowish deposits contain $NiCl_2 \cdot 6H_2O$. Similar results were found in Chen *et al.*'s previous work [3] as well. It is presumed that HCl reacted with metallic Ni and formed the deposition precursor $NiCl_2$. The gaseous $NiCl_2$ precursor originated from the vaporization of the added $NiCl_2$ and the HCl reaction was carried into the fluidized bed with the flowing gases. Since the temperature in the fluidized bed region was lower, $NiCl_2$ was reduced with H_2, and Ni was thus formed and deposited on the alumina particles. If the temperature of the upper furnace increased, the tendency of the
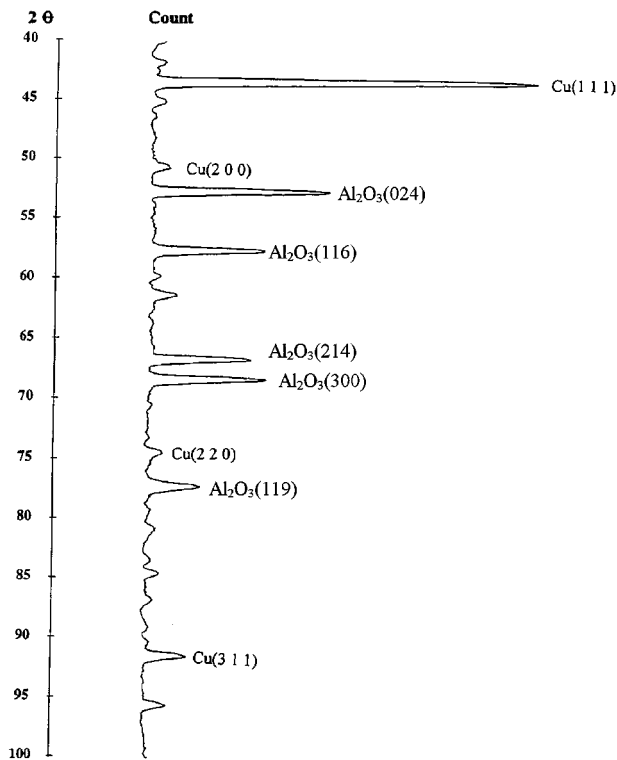
Figure 9 The XRD result of the Cu-deposited alumina particles from experiment 16.

Figure 10 The SEM secondary electron image of surface morphology of the Cu-deposited alumina particle from experiment 16.

$NiCl_2$ reduction reaction on the alumina surface would decrease. The non-decomposed $NiCl_2$ gas condensed on the glass substrates, absorbed moisture and formed $NiCl_2 \cdot 6H_2O$. Sanjurjo *et al.* found that HCl gas reacted with metals and formed chlorides as the deposition precursors in most of their work [11–14]. Kuznetsov *et al.* [20] and Uemura et al. [21] used $NiCl_2$ as the deposition source and successfully deposited metallic Ni onto the substrates. Busey and Giauque [22] and Williams *et al.* [23] studied the thermodynamics and kinetics of the reaction that metallic Ni formed from the nickel chloride reduction with hydrogen. Although the mechanisms of chemical vapor deposition of Ni onto alumina have not been investigated in this study, the above-mentioned presumption of the formation of $NiCl_2 \cdot 6H_2O$ is in agreement with the work found in the above-mentioned literature [20–23].

Cu deposition on alumina particles was carried out as well using the CVD-CFBR technique. For the experiment 16 as listed in Table I, 5 wt% of CuCl was added, and the temperatures of the upper and the lower furnaces were 675°C and 725°C, respectively. After 3 hours' reaction, the originally brownish alumina particles turned into a color of red-brown. The inner wall of the quartz reactor had a red-brownish coating as well. The XRD analysis result shown in Fig. 9 indicated that the red-brown deposits were metallic Cu. The deposited Cu on the alumina surface displayed an island-like morphology as shown in Fig. 10. Based on the results of experiments 17–24, a conclusion similar to that of the Ni-deposition experiments could be drawn that the thickness of Cu deposition layer increased with a higher amount of CuCl addition and higher temperature of the lower furnace as well.

Experiments 17, 22, 23, and 24 were carried out in similar conditions with various upper furnace temperatures, 675°C, 700°C, 750°C, and 775°C, respectively. The thickness of the metallic Cu layers decreased with increasing temperature of the upper furnace. As for experiment 24, when the temperature of the upper furnace was 775°C, some green-color deposits were formed both on the inner walls of the reactor and the cyclone. The XRD result shown in Fig. 11 indicates that the deposits are CuCl. It is presumed that the deposited CuCl is formed from the condensation of the non-decomposed deposition precursor, gaseous CuCl. Similar to the formation mechanism of gaseous $NiCl_2$, the gaseous CuCl could be formed by the reaction between
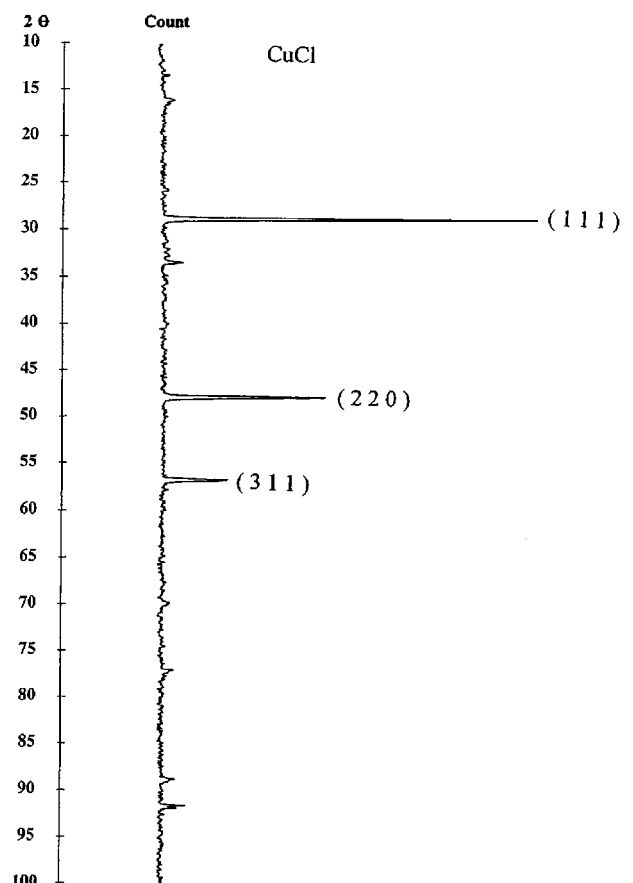

Figure 11 The XRD result of the green-color deposits from experiment 24.

HCl and Cu or from the vaporization of the added CuCl.

4. Conclusion

Metallic Ni and Cu have been successfully deposited onto alumina particles of 45 μm diameter by using the CVD-CFBR technology. The elutriated alumina particles from the reactor were collected and circulated back to the reactor. The rates of metal deposition increased with the amount of addition of their respective chlorides, and the rates also increased if the temperature of the lower furnace (the formation region of the deposition precursor) was increased.

Acknowledgements

References

1. K. N. STRAFFORD, P. K. DATTA and C. G. GOOGAN (eds.), "Coating and Surface Treatment for Corrosion and Wear Resistance" (Ellis Horwood Limited, Chichester, England, 1984).
2. L. PAWLOWSKI, "The Science and Engineering of Thermal Spray Coatings" (John Wiley & Sons, New York, 1995).
3. C.-C. CHEN and S.-W. CHEN, *J. Mater. Sci.* **32** (1997) 4429.
4. C.-C. CHEN, S.-W. CHEN and Y.-W. YEN, "in AIChE Symposium Series, Vol. 92: Progress in Fluidization and Fluid Particle Systems," edited by D. King, (AIChE, New York, 1996), 96.
5. J. M. BLOCHER, JR., US Patent no. 3249509 (1966).
6. J. L. KAAE, *Ceram. Eng. Sci. Proc.* **9**(9-10) (1988) 1159.
7. A. SANJURJO, M. C. H. McKUBRE and G. D. CRAIG, *Surf. Coat. Tech.* **39/40** (1989) 691.
8. S. MOROOKA, T. OKUBO and K. KUSAKABE, Powder Tech. **63** (1990) 105.
9. I. KIMURA, N. HOTTA, J.-I., NIWANO and M. TANAKA, *ibid.* **68** (1991)153.
10. A. SANJURJO, B. J. WOOD, K. H. LAU, G. T. TONG, D. K. CHOI, M. C. H. McKUBRE, H. K. SONG, D. PETERS and N. CHURCH, *Surf. Coat. Tech.* **49** (1991) 103.
11. A. SANJURJO, B. J. WOOD, K. H. LAU, G. T. TONG, D. K. CHOI, M. C. H. McKUBRE, H. K. SONG and N. CHURCH, *ibid.*110.
12. B. J. WOOD, A. SANJURJO, G. T. TONG and S. E. SWIDER, *ibid.* 228.
13. A. SANJURJO, K. LAU and B. WOOD, *ibid.* **54/55** (1992) 219.
14. K. H. LAU, A. SANJURJO and B. J. WOOD, *ibid.* 234.
15. A. SANJURJO and B. J. WOOD US Patent no 5171734 (1992).
16. K. TSUGEKI, T. KATO, Y. KOYANAGI, K. KUSAKABE and S. MOROOKA *J. Mater. Sci.* **28** (1993) 3168.
17. S. KINKEL, G. N. ANGELOPOULOS and W. DAHL, *Surf. Coat. Tech.* **64** (1994) 119.
18. R. W. REYNOLDSON, Industrial Heating, (September, 1994) 126.
19. A.-J. CHANG, S.-W. RHEE and S. BAIK, *J. Mater. Sci.* **30** (1995) 1180.
20. G. D. KUZNETSOV, A. A. BABAD-ZAKHRYAPIN and V. F. GVOZD, *Z. Metall.* **8**(5) (1972) 618.
21. Y. UEMURA, Y. HATATE and A. IKARI, *J. Che. Eng. Jap.* **22**(1) (1989) 48.
22. R. H. BUSEY and W. F. GIAUQUE, *J. Amer. Chem. Soc.* **75** (1953) 1791.
23. D. T. WILLIAMS, S. K. EL-RAHAIBY and Y. K. RAO, *Metall. Trans. B* **12B** (1981) 161.